JOURNAL OF GUIDANCE, CONTROL, AND DYNAMICS
Vol. 16, No. 6, November–December 1993

Optimal Cooperative Power-Limited Rendezvous Between Neighboring Circular Orbits

Victoria Coverstone-Carroll and John E. Prussing
University of Illinois at Urbana-Champaign, Urbana, Illinois 61801

A minimum-fuel rendezvous of two power-limited spacecraft is investigated. Both vehicles are active and provide thrust to complete the rendezvous. Total propellant consumption is minimized. Analytical solutions are obtained for cooperative rendezvous in the linearized Hill-Clohessy-Wiltshire gravity field. The optimal solutions depend in a complicated way on the power-to-mass ratios of the spacecraft, the initial orbits, and the specified transfer time. For comparison purposes, analytical solutions for active-passive rendezvous in the linearized gravity field are also determined. Cooperative rendezvous requires smaller total propellant consumption, resulting in greater payload capability.

Introduction

HISTORICALLY, spacecraft rendezvous involves one thrusting (active) vehicle and one coasting (passive) vehicle. A cooperative power-limited (PL) rendezvous is an orbital maneuver in which two PL spacecraft are thrusting, allowing a reduction in total propellant consumption when compared with the traditional active-passive rendezvous.

Early studies of cooperative rendezvous considered general linear or nonlinear systems with various performance indices. Meschler[1] discussed the minimum-time cooperative rendezvous between two linear time-varying systems with bounded control input. Gieseking[2] studied the single and multi-input rendezvous problem with the Lagrangian cost functional being the integral-squared-error plus weighted control effort. Carter[3] considered cooperative rendezvous using linear systems with a quadratic cost functional in terms of the state error and control and obtained a fixed-coefficient feedback control law. Kahne[4] derived the necessary conditions for a cooperative state rendezvous for two general nonlinear systems and for a general performance index in the Lagrangian form.

Recently, cooperative rendezvous methodology has been applied to spacecraft maneuvering. Prussing and Conway[5] determined the optimal terminal maneuver for a cooperative impulsive rendezvous. Mirfakhraie[6] and Mirfakhraie and Conway[7] developed a method for determining optimal fuel-minimizing trajectories for the fixed-time impulsive cooperative rendezvous. This paper determines propellant minimizing trajectories for the fixed-time cooperative rendezvous of two power-limited spacecraft. The spacecraft are initially in neighboring circular orbits; hence the Hill-Clohessy-Wiltshire linearized gravity field is used to approximate the inverse-square gravity field. With the linearized gravity model, analytic solutions to the necessary conditions for optimality are obtained. Optimal cooperative and active-passive solutions are presented for different initial orbits and for various transfer times and maximum exhaust powers. The spacecraft are presumed to be identical in initial mass and maximum engine exhaust power.

Necessary Conditions for an Optimal Solution

Power-limited spacecraft have propulsion systems that have an upper bound on the exhaust power P_{max} that the engine can supply. Typically, P_{max} is set by the limitations of a power source that is separate from the engines. The equations of motion for PL spacecraft subject to a single gravitational

Victoria Coverstone-Carroll is an assistant professor of aeronautical and astronautical engineering at the University of Illinois at Urbana-Champaign. Her current research interests include optimal low-thrust spacecraft trajectories and autonomous adaptive control. She was the recipient of the ZONTA Amelia Earhart Award and was a NASA Consortium Fellow. She is a member of the American Astronautical Society and AIAA.

John E. Prussing is a professor of aeronautical and astronautical engineering at the University of Illinois at Urbana-Champaign, where he has been a faculty member since 1969. He received his B.S. and M.S. degrees in 1963 in aeronautics and astronautics from the Massachusetts Institute of Technology and his Sc.D. in instrumentation from MIT in 1967. He is a past associate editor of the *Journal of Guidance, Control, and Dynamics* and is coauthor of the text *Orbital Mechanics* published in 1993. He is an Associate Fellow of AIAA, has chaired the AIAA Astrodynamics Technical Committee, and was technical chairman of three AIAA astrodynamics conferences.

Received July 10, 1992; revision received Jan. 20, 1993; accepted for publication Feb. 12, 1993.

source along with an equation for the mass change along a thrusting trajectory were derived by Prussing[8]:

$$\ddot{r}_i = g(r_i) + \Gamma_i \qquad i = 1, 2 \tag{1}$$

$$\frac{1}{m(t)} - \frac{1}{m(t_0)} = \int_{t_0}^{t} \frac{\Gamma^2}{2P}\,dt \tag{2}$$

where r is the position vector, $g(r)$ the gravitational acceleration, Γ the thrust acceleration, and m the mass of the vehicle. Equation (2) indicates that the final mass of a vehicle is maximized for a control history $\Gamma(t)$ when the engine is operating at $P_{\max}$ since any smaller exhaust power would result in a greater change in the total mass of the vehicle for the same trajectory satisfying the equations of motion (1).

For convenience, a new variable α, the power-to-mass (PTM) ratio, is defined as follows:

$$\alpha(t) = P_{\max}/m(t) \tag{3}$$

The introduction of the new variable α allows Eq. (2) to be written in an alternative way:

$$\dot{\alpha} = \Gamma^2/2 \tag{4}$$

For a single vehicle, labeled vehicle i, define a state vector x_i of dimension 7×1, $x_i^T = [r_i^T \quad \dot{r}_i^T \quad \alpha_i]$. The equations of motion for the ith vehicle can then be written in first-order differential form:

$$\dot{x}_i^T = f_i^T[x_i(t), \Gamma_i(t)] = [\dot{r}_i^T \quad g^T(r_i) + \Gamma_i^T \quad \tfrac{1}{2}\Gamma_i^T\Gamma_i]^T \tag{5}$$

For two active spacecraft, a combined state vector x of dimension 14×1, $x^T = [r_1^T\ \dot{r}_1^T \alpha_1\ r_2^T\ \dot{r}_2^T\ \alpha_2] = [x_1^T\ x_2^T]$, and a control vector Γ of dimension 6×1, $\Gamma^T = [\Gamma_1^T\ \Gamma_2^T]$, are defined. The equations of motion then can be described by two sets of uncoupled equations, each of the form shown in Eq. (5):

$$\dot{x}^T = [f_1^T(x_1, \Gamma_1) \quad f_2^T(x_2, \Gamma_2)] = f^T[x(t), \Gamma(t)] \tag{6}$$

The objective of an optimal cooperative rendezvous is to transfer each vehicle from its initial orbit to a common final position and velocity in a given amount of time while maximizing the sum of the final masses of the spacecraft. Equation (7) relates this objective in terms of the reciprocal to the PTM ratios. The subscript f on a variable denotes the variable evaluated at the final time:

$$J = -\sum_{i=1}^{2} m_{i_f} = -\sum_{i=1}^{2} \frac{P_{\max_i}}{\alpha_{i_f}} = \phi[x(t_f)] \tag{7}$$

The six terminal constraints on the final position and velocity of the two vehicles $\psi[x(t_f)]$ are considered by defining a function Φ in the manner described by Bryson and Ho[9]:

$$\Phi[x(t_f)] = \phi[x(t_f)] + \nu^T\psi[x(t_f)] \tag{8}$$

where $\phi[x(t_f)]$ is defined by Eq. (7) and $\psi[x(t_f)]$ is given as

$$\psi^T[x(t_f)] = (r_{1_f}^T - r_{2_f}^T,\ \dot{r}_{1_f}^T - \dot{r}_{2_f}^T) \tag{9}$$

and ν is a 6×1 vector of parameters. After substituting Eqs. (7) and (9) into Eq. (8), Φ can be represented as

$$\Phi = -\sum_{i=1}^{2} \frac{P_{\max_i}}{\alpha_{i_f}} + \nu_1^T(r_{1_f} - r_{2_f}) + \nu_2^T(\dot{r}_{1_f} - \dot{r}_{2_f}) \tag{10}$$

The equation for the cost functional, Eq. (7), depends only on the terminal states of the system. The Hamiltonian for this system can be simply expressed by

$$H = \lambda^T(t) f[x(t), \Gamma(t)] \tag{11}$$

where $\lambda(t)$ is the 14×1 costate vector and can be partitioned into two similar 7×1 vectors of costates:

$$\lambda^T(t) = [\lambda_1^T(t),\ \lambda_2^T(t)]$$

$$\lambda_i^T(t) = [\lambda_{r_i}^T(t),\ \lambda_{\dot{r}_i}^T(t),\ \lambda_{\alpha_i}(t)] \qquad i = 1, 2 \tag{12}$$

Equations (5), (6), (11), and (12) may be used to write the Hamiltonian compactly as

$$H = \sum_{i=1}^{2} \{\lambda_{r_i}^T\dot{r}_i + \lambda_{\dot{r}_i}^T[g(r_i) + \Gamma_i] + \tfrac{1}{2}\lambda_{\alpha_i}\Gamma_i^T\Gamma_i\} \tag{13}$$

The necessary conditions for a minimum of J are found through optimal control theory as outlined in Ref. 9. The necessary conditions comprise 28 differential equations. Fourteen of these are the equations of motion given by Eq. (6) that must be satisfied along an optimal solution. The initial conditions on the state $x(t_0)$ that include positions, velocities, and PTM ratios of both vehicles at the beginning of the maneuver are known. The remaining 14 differential equations involve the costate variables. The costate differential equations given by Eqs. (14) must also be satisfied along an optimal solution; the final conditions on the costates are supplied by Eqs. (15):

$$\dot{\lambda} = -\left[\frac{\partial f}{\partial x}\right]^T \lambda \tag{14a}$$

for 14 differential equations or

$$\dot{\lambda}_{r_i} = -G^T(r_i)\lambda_{\dot{r}_i} \tag{14b}$$

for six differential equations where $i = 1, 2$, and $G(r_i) = [\partial g(r_i)/\partial r_i]$,

$$\dot{\lambda}_{\dot{r}_i} = -\lambda_{r_i} \tag{14c}$$

for six differential equations where $i = 1, 2$,

$$\dot{\lambda}_{\alpha_i} = 0 \tag{14d}$$

for two differential equations where $i = 1, 2$, with

$$\lambda^T(t_f) = \frac{\partial \Phi}{\partial x(t_f)} \tag{15a}$$

for 14 boundary conditions or

$$\lambda_{r_i}(t_f) = (-1)^{i+1}\nu_1 \quad \text{for} \quad i = 1, 2 \tag{15b}$$

for six boundary conditions,

$$\lambda_{\dot{r}_i}(t_f) = (-1)^{i+1}\nu_2 \quad \text{for} \quad i = 1, 2 \tag{15c}$$

for six boundary conditions,

$$\lambda_{\alpha_i}(t_f) = P_{\max_i}/\alpha_{i_f}^2 \tag{15d}$$

for two boundary conditions.

The optimality condition states that along an optimal solution the control vector is chosen to minimize the Hamiltonian of Eq. (13). The optimal control direction and magnitude for the vehicles are supplied through the costate variables by

$$\left(\frac{\partial H}{\partial \Gamma}\right)^T = \left(\frac{\partial f}{\partial \Gamma}\right)^T \lambda = 0 \tag{16a}$$

for six algebraic equations or

$$\Gamma_i = -(\lambda_{\dot{r}_i}/\lambda_{\alpha_i}) \tag{16b}$$

for six algebraic equations where $i = 1, 2$.

The 28 differential equations given by Eqs. (6) and (14) along with the 28 split boundary conditions form a two-point

boundary-value problem (TPBVP). The six parameters ν are found to satisfy the six terminal constraints of Eq. (9). The six elements of the control vector Γ are determined through Eqs. (16). Although, in general, the TPBVP may be difficult to solve analytically, an integral of the solution is found by noticing that $f[x(t), \Gamma(t)]$ is not an explicit function of t that guarantees that the Hamiltonian given by Eq. (18) is constant along the optimal trajectory.[9]

Equation (16) states that the optimal thrust acceleration Γ_i is in the opposite direction of the ith velocity costate vector. Lawden[10] defined the negative of this velocity costate vector to be the primer vector p_i. Equations (16) and (17) can be combined to show that the optimal thrust direction for each vehicle is always in the direction of that vehicle's primer vector:

$$p_i(t) = -\lambda_{r_i}(t) \tag{17}$$

$$\Gamma_i = p_i/\lambda_{\alpha_i} = \alpha_{i_f}^2 p_i/P_{\max_i} \tag{18}$$

for six algebraic equations where $i = 1, 2$.

Hill-Clohessy-Wiltshire Linearized Gravity Model

The Hill-Clohessy-Wiltshire gravity field is a linear approximation to the inverse-square gravity field. The linearization is performed relative to a circular reference orbit of radius r^*. The current relative position and velocity of the spacecraft are expressed with respect to a rotating reference frame whose origin lies in the circular reference orbit.

To demonstrate the linearization, consider the current position $r(t)$ of the vehicle as a perturbation $\delta r(t)$ away from r^*. The vector r^* locates the origin of the rotating reference frame. Each vehicle's equation of motion (1) can then be written as

$$\ddot{r}^* + \delta\ddot{r}_i = g(r^* + \delta r_i) + \Gamma_i \qquad i = 1, 2 \tag{19}$$

where

$$g(r_i) = -(\mu r_i/r_i^3)$$

where $i = 1, 2$, and μ = gravitational constant. The gravity vector $g(r_i)$ is expanded in a Taylor series about the reference orbit, and second and higher order terms in the expansion are neglected. Equation (19) then becomes

$$\ddot{r}^* + \delta\ddot{r}_i = g(r^*) + G(r^*)\delta r_i + \Gamma_i \qquad i = 1, 2 \tag{20}$$

where

$$G(r^*) = \left[\frac{\partial g(r)}{\partial r}\right]_{r=r^*} = \left[\frac{\mu}{r^5}(3rr^T - r^2 I_3)\right]_{r=r^*} = G^T(r^*) \tag{21}$$

where $I_3 = 3 \times 3$ identity matrix.
The reference orbit satisfies its own equation of motion:

$$\ddot{r}^* = g(r^*) \tag{22}$$

Subtracting Eq. (22) from Eq. (20), one represents the relative motion by a linear second-order differential equation:

$$\delta\ddot{r}_i = G(r^*)\delta r_i + \Gamma_i \qquad i = 1, 2 \tag{23}$$

Expressing Eq. (23) in the rotating reference frame, referred to as the Hill-Clohessy-Wiltshire (CW) frame, the equations of relative motion become[11]

$$\delta\ddot{r}_{iR} = A\,\delta r_i + B\delta\dot{r}_{iR} + \Gamma_i$$

$$\delta r_i^T = (x_i, y_i, z_i)$$

$$A = \begin{bmatrix} 3n^2 & 0 & 0 \\ 0 & 0 & 0 \\ 0 & 0 & -n^2 \end{bmatrix} \quad : \quad B = \begin{bmatrix} 0 & 2n & 0 \\ -2n & 0 & 0 \\ 0 & 0 & 0 \end{bmatrix} \tag{24}$$

The variable x_i is measured along the radius vector r^*. The coordinate y_i is measured along the local horizontal with positive y being in the direction of motion of the reference frame. The coordinate z_i completes the right-hand coordinate system and is normal to the reference orbit. The subscript R in Eq. (24) denotes that time derivatives are with respect to the rotating coordinate system. The mean motion of the circular reference orbit n, which appears in the matrices A and B, is $n = (\mu/r^{*3})^{1/2}$.

Optimal Cooperative Rendezvous

The necessary conditions indicate that each vehicle's optimal thrust vector is in the direction of its respective primer vector. The necessary conditions also yield that both primer vectors satisfy the same homogeneous differential equation as the relative position vectors.[12] Therefore, the state transition matrix for the primer vector Φ_{pp} is the same transition matrix that propagates the relative position and velocity vectors Φ_{rr} of a passive vehicle. The primer vector differential equation is

$$\ddot{p}_i = Ap_i + B\dot{p}_i; \qquad i = 1, 2 \tag{25}$$

To determine the optimal cooperative rendezvous solution, define a new 24×1 state variable y:

$$y^T = [y_1^T\, y_2^T]; \quad y_i^T = [\delta r_\delta^T\, \dot{r}_i^T\, p_i^T\, \dot{p}_i^T] = [y_{i1}^T\, y_{i2}^T]; \quad i = 1, 2 \tag{26}$$

The new state y_i satisfies the linear constant coefficient differential equation, where $i = 1, 2$,

$$\dot{y}_i = \begin{bmatrix} 0_3 & I_3 & 0_3 & 0_3 \\ A & B & \dfrac{\alpha_{i_f}^2}{P_{\max_i}} I_3 & 0_3 \\ 0_3 & 0_3 & 0_3 & I_3 \\ 0_3 & 0_3 & A & B \end{bmatrix} y_i \tag{27}$$

Equation (27) has the solution given in Eqs. (28–31). The variables Φ_{rr}, Φ_{rp}, and Φ_{pp} are 6×6 partitions of the state transition matrix and are given in the Appendix. The vehicle's primer and primer rate are supplied in Eq. (29). The boundary conditions in Eq. (29) show that the primer vector of vehicle 1 is equal in magnitude but opposite in direction to the primer vector of vehicle 2 for all time. The vehicle's relative position and velocity vectors are given in Eq. (30).

$$y_i(t) = \begin{bmatrix} \Phi_{rr}(t - t_0) & \dfrac{\alpha_{i_f}^2}{P_{\max_i}} \Phi_{rp}(t - t_0) \\ 0_6 & \Phi_{pp}(t - t_0) \end{bmatrix} \begin{bmatrix} y_{i1}(t_0) \\ y_{i2}(t_0) \end{bmatrix} \qquad i = 1, 2 \tag{28}$$

or

$$\begin{bmatrix} p_i(t) \\ \dot{p}_i(t) \end{bmatrix} = \Phi_{pp}(t - t_0) \begin{bmatrix} p_i(t_0) \\ \dot{p}_i(t_0) \end{bmatrix}$$

$$= \Phi_{pp}(t - t_0)\Phi_{pp}^{-1}(t_f - t_0) \begin{bmatrix} p_i(t_f) \\ \dot{p}_i(t_f) \end{bmatrix} \tag{29a}$$

$$\begin{bmatrix} p_i(t_f) \\ \dot{p}_i(t_f) \end{bmatrix} = \begin{bmatrix} (-1)^i \nu_2 \\ (-1)^{i+1}(\nu_1 - B\nu_2) \end{bmatrix} \tag{29b}$$

$$\begin{bmatrix}\delta r_i(t)\\ \delta \dot{r}_i(t)\end{bmatrix} = \Phi_{rr}(t-t_0)\begin{bmatrix}\delta r_i(t_0)\\ \delta \dot{r}_i(t_0)\end{bmatrix}$$

$$+ \frac{\alpha_{i_f}^2}{P_{\max_i}}\Phi_{rp}(t-t_0)\Phi_{pp}^{-1}(t_f-t_0)\begin{bmatrix}p_i(t_f)\\ \dot{p}_i(t_f)\end{bmatrix} \tag{30}$$

As previously stated, the values of the parameters ν are determined by enforcing the terminal constraints:

$$\nu_1 = \left(\frac{\alpha_{1_f}^2}{P_{\max_1}} + \frac{\alpha_{2_f}^2}{P_{\max_2}}\right)^{-1}[B \quad -I_3]\Phi_{pp}(T)c$$

$$\nu_2 = \left(\frac{\alpha_{1_f}^2}{P_{\max_1}} + \frac{\alpha_{2_f}^2}{P_{\max_2}}\right)^{-1}[I_3 \quad 0_3]\Phi_{pp}(T)c$$

where

$$\Delta r_0 = \delta r_1(t_0) - \delta r_2(t_0) \tag{31a}$$

$$\Delta \dot{r}_0 = \delta \dot{r}_1(t_0) - \delta \dot{r}_2(t_0) \tag{31b}$$

$$T = t_f - t_0 \tag{31c}$$

$$c = \Phi_{rp}^{-1}(T)\Phi_{rr}(T)\begin{bmatrix}\Delta r_0\\ \Delta \dot{r}_0\end{bmatrix} \tag{31d}$$

Equation (4) can be integrated to yield an expression for the final PTM ratios. Four new scalar constants a, b_1, b_2, and b_3 and a constant matrix K have been defined for convenience (the matrix K can be found in the Appendix):

$$\alpha_{1_f} = \alpha_1(t_0)\left[1 + \frac{b_3^2 b_2}{(b_3+a^2)^2}\right] \tag{32a}$$

$$\alpha_{2_f} = \alpha_2(t_0)\left[1 + \frac{a^4 b_2}{b_1(b_3+a^2)^2}\right] \tag{32b}$$

$$b_1 = \frac{\alpha_2(t_0)}{\alpha_1(t_0)} \quad : \quad b_2 = \frac{c^T K c}{2\alpha_1(t_0)} \quad : \quad b_3 = \frac{P_{\max_2}}{P_{\max_1}} \tag{32c}$$

$$K = \int_{t_0}^{t_f} \Phi_{pp}^T(t)\begin{bmatrix}I_3 & 0_3\\ 0_3 & 0_3\end{bmatrix}\Phi_{pp}(t)\,dt \tag{32d}$$

$$a = \alpha_{2_f}/\alpha_{1_f} \tag{32e}$$

Inserting the two α equations into the definition of the nondimensional parameter a given by Eq. (32e) results in a fifth-degree polynomial in terms of the unknown a:

$$a^5 - (b_1+b_2)a^4 + 2b_3a^3 - 2b_3b_1a^2 + b_3^2(1+b_2)a - b_3^2b_1 = 0 \tag{33}$$

Note that the zeros of this polynomial are functions of the initial PTM ratios, the total maneuver time, and the initial position and velocity of the vehicles. Since a represents the ratio of final PTM ratios, only positive real zeros of Eq. (33) have physical significance. If more than one zero is positive and real, the value of a that minimizes the total propellant consumption is chosen. This minimizing zero results in Eq. (34) having its most negative value. Equation (34) is derived from Eq. (7) with the use of Eqs. (32).

$$J_c = -\frac{m_{1_0}(b_3+a)(b_3+a^2)^2}{a[(b_3+a^2)^2 + b_3^2 b_2]} \tag{34}$$

Using the minimizing zero, the individual PTM ratios are given by Eqs. (32). The optimal thrust acceleration vectors are given by Eq. (35), which reveals that in general both vehicles are thrusting in opposite directions throughout the entire maneuver:

$$\Gamma_1 = \frac{-b_3[I_3\ 0_3]\Phi_{pp}(t)c}{(b_3+a^2)}$$

$$\Gamma_2 = -(a^2/b_3)\,\Gamma_1 \tag{35}$$

The relative position and velocity of both spacecraft are expressed in Eq. (36). The mass history is determined through the individual PTM ratios of each vehicle as is indicated in Eq. (37):

$$\left[\delta r_1^T(t)\delta \dot{r}_1^T(t)\right]^T = \Phi_{rr}(t)\left[\delta r_1^T(t_0)\delta \dot{r}_1^T(t_0)\right]^T - \frac{b_3\Phi_{rp}(t)c}{(b_3+a^2)}$$

$$\left[\delta r_2^T(t)\delta \dot{r}_2^T(t)\right]^T = \Phi_{rr}(t)\left[\delta r_2^T(t_0)\delta \dot{r}_2^T(t_0)\right]^T + \frac{a^2\Phi_{rp}(t)c}{(b_3+a^2)} \tag{36}$$

$$m_i(t) = [P_{\max_i}/\alpha_i(t)] \qquad i = 1, 2 \tag{37}$$

Using Eqs. (36), the final position and velocity of the two spacecraft expressed in the CW frame can be written as a convex combination of the initial positions and velocities of the spacecraft propagated forward in time by the state transition matrix Φ_{rr}. Equation (38) can be used to predict the optimal final orbit:

$$\begin{bmatrix}\delta r_i(T)\\ \delta \dot{r}_i(T)\end{bmatrix} = \frac{1}{b_3+a^2}\Phi_{rr}(T)\begin{bmatrix}a^2\delta r_1(t_0) + b_3\delta r_2(t_0)\\ a^2\delta \dot{r}_1(t_0) + b_3\delta \dot{r}_2(t_0)\end{bmatrix} \quad i = 1, 2 \tag{38}$$

Active-Passive Rendezvous Solution

With only one active vehicle and a fixed maneuver time, the final position and velocity of both vehicles are easily supplied by propagating the passive vehicle along its initial orbit. Throughout the analysis and without loss of generality, vehicle 1 will be the passive vehicle. Vehicle 1's relative position and velocity with respect to the rotating reference frame are given through the state transition matrix $\Phi_{rr}(t-t_0)$. Vehicle 2 does thrust, and the optimal thrust acceleration is given by Eq. (40):

$$\begin{bmatrix}\delta r_1(t)\\ \delta \dot{r}_1(t)\end{bmatrix} = \Phi_{rr}(t-t_0)\begin{bmatrix}\delta r_1(t_0)\\ \delta \dot{r}_1(t_0)\end{bmatrix} \tag{39}$$

$$\Gamma_2(t) = [I_3 \quad 0_3]\Phi_{pp}(t-t_0)c \tag{40}$$

The vector c is the same vector described in Eqs. (31). Equation (40) shows that the optimal thrust acceleration is independent of the initial PTM ratio. Using the optimal thrust acceleration for vehicle 2, one can show that the relative position and velocity with respect to the rotating reference frame is

$$\begin{bmatrix}\delta r_2(t)\\ \delta \dot{r}_2(t)\end{bmatrix} = \Phi_{rr}(t-t_0)\begin{bmatrix}\delta r_2(t_0)\\ \delta \dot{r}_2(t_0)\end{bmatrix} + \Phi_{rp}(t-t_0)c \tag{41}$$

Vehicle 1 expends no propellant for this maneuver. Vehicle 2's final mass is contained in the final PTM ratio given by Eq. (42):

$$\alpha_{2_f} = \alpha_2(t_0) + \tfrac{1}{2}c^T K c = \alpha_1(t_0)(b_1+b_2) \tag{42}$$

The cost functional (7) for the active-passive rendezvous can be written as

$$J_n = -\frac{m_{1_0}(b_1+b_2+b_3)}{b_1+b_2} \tag{43}$$

As was shown in Eq. (40), for given initial positions and velocities of the vehicles and a fixed total maneuver time, a

unique optimal thrust acceleration vector Γ_2 exists that will transport an active vehicle to a passive vehicle. The total change in the PTM ratio is constant for this active-passive maneuver:

$$\Delta\alpha = \alpha_f - \alpha_0 = \frac{1}{2}\int_{t_0}^{t_f} \Gamma(\tau)^T\Gamma(\tau)\, d\tau$$

$$= \frac{1}{2}\int_{t_0}^{t_f} p(\tau)^T p(\tau)\, d\tau = K_{nc} \tag{44}$$

If one defines ΔM_n as the total propellant consumed for an active-passive rendezvous where the subscript n denotes a noncooperative rendezvous, then ΔM_n may be written in terms of K_{nc} supplied by Eq. (44), the maximum exhaust power $P_{\max}$, and the initial PTM ratio α_0 of the thrusting vehicle. Either Eq. (43) or Eq. (45) may be used as the cost functional for an active-passive rendezvous since they are simply related by the additive constant of the sum of spacecraft initial masses:

$$\Delta M_n = \frac{P_{\max} K_{nc}}{\alpha_0(K_{nc} + \alpha_0)} \tag{45}$$

Once an optimal active-passive solution has been obtained for given initial positions and velocities, total maneuver time, and α_0, the optimal noncooperative solution is known for all α_0. Equation (41) indicates that the active vehicle's optimal position and velocity histories are independent of the α_0. Let $\Delta M_{n\,\text{old}}$ represent the total propellant consumed to perform the rendezvous with an initial PTM ratio $\alpha_{0\,\text{old}} = P_{\max\,\text{old}}/m_{0\,\text{old}}$. The total propellant consumed $\Delta M_{n\,\text{new}}$ for the same rendezvous with a new PTM ratio $\alpha_{0\,\text{new}} = P_{\max\,\text{new}}/m_{0\,\text{new}}$ can then be obtained through Eq. (46):

$$\Delta M_{n\,\text{new}} = m_{0\,\text{new}} - \frac{P_{\max\,\text{new}}(m_{0\,\text{old}} - \Delta M_{n\,\text{old}})}{(\alpha_{0\,\text{new}} - \alpha_{0\,\text{old}})(m_{0\,\text{old}} - \Delta M_{n\,\text{old}}) + P_{\max\,\text{old}}} \tag{46}$$

Assumptions

Optimal cooperative rendezvous solutions are influenced by 15 parameters: 2 position and velocity vectors, 2 PTM ratios, and the total maneuver time. With equal initial PTM ratios, the optimal solutions tend to be very cooperative, i.e., both vehicles play a large part in the rendezvous. With unequal initial PTM ratios, one vehicle provides the majority of thrust and the optimal solution moves toward an active-passive rendezvous.[12] Therefore, to insure the maximum involvement of each vehicle, identical vehicles will be assumed. Power-limited vehicles with maximum exhaust powers $P_{\max}$ of approximately 10^7 W and initial masses of 1000 kg are anticipated. In canonical units, a spacecraft in a circular orbit of radius 1 distance unit (DU) has an orbital period of 2π time units (TU). The maximum exhaust power and initial mass previously stated translate to an initial PTM ratio of $\alpha_0 = 0.129$ in Earth canonical units, 3.668 in lunar canonical units, and 56.6 in heliocentric canonical units. These three PTM ratios are used exclusively.

The initial orbits are circular. The radius of vehicle 1's orbit, r_{10}, is 1 DU. The orbital radius of vehicle 2, r_{20}, and the phase angle between the vehicles is varied. Although numerical results for near-circular initial orbits are not supplied, the analytic solutions obtained for both the cooperative and active-passive rendezvous are applicable to these initial orbits. Near-circular orbits possess a small velocity component in the radial direction. A cooperative rendezvous between neighboring coplanar orbits is considered first. A neighboring inclined rendezvous is discussed in the subsequent section.

Neighboring Coplanar Rendezvous Results

Effects on total propellant consumption of varying the initial PTM ratio α_0, the total rendezvous time T, and the initial phase angle ϕ_0 between the two vehicles are examined. For both cooperative and active-passive rendezvous, the following trends are observed. As the total rendezvous time T is increased, the cost of the rendezvous decreases. As α_0 is increased, the relative efficiency of the engines increases and the cost decreases. Also, in all cases, cooperative rendezvous requires less total propellant than active-passive rendezvous. However the percentage of savings in propellant consumed is a function of T, ϕ_0, $\Delta r_0 = r_{10} - r_{20}$, and α_0. In general, cooperative rendezvous offers the most savings over an active-passive rendezvous for high α_0 and large T. For small α_0 or small T, the optimal cooperative rendezvous moves toward a noncooperative maneuver. This behavior can be explained by examining the zeros of the fifth-degree polynomial given in Eq. (33). For identical vehicles, $b_1 = b_3 = 1$ as defined in Eqs. (32) and the polynomial simplifies to Eq. (47), which has the five zeros given in Eqs. (48)[13]:

$$a^5 - (1 + b_2)a^4 + 2a^3 - 2a^2 + (1 + b_2)a - 1 = 0 \tag{47}$$

$$a = 1$$

$$a = \frac{b_2/4 \pm \sqrt{-4 + [-(b_2/2) - \sqrt{b_2 + (b_2^2/4)}]^2} + \sqrt{b_2 + (b_2^2/4)}}{2}$$

$$a = \frac{b_2/4 \pm \sqrt{-4 + [-(b_2/2) + \sqrt{b_2 + (b_2^2/4)}]^2} - \sqrt{b_2 + (b_2^2/4)}}{2} \tag{48}$$

One zero is always $a = 1$ and represents the solution where both vehicle final masses are equal. Next, note that for values of b_2 between $0 \le b_2 < 4/3$, the only real zero of the polynomial is $a = 1$. For values of $b_2 > 4/3$, three real zeros are obtained. Two of the zeros are locally minimizing values of the cost given in Eq. (34). The third zero represents a locally maximizing solution. For the special case where $b_2 = 4/3$, all three real zeros degenerate to the $a = 1$ minimizing solution. Now, recall the definition for b_2 from Eq. (32c). The variables c and K are functions of the initial positions and velocities of the vehicles and the total maneuver time. Numerical calculations show that in general b_2 decreases in value with increasing T and increasing α_0. Therefore, for sufficiently large α_0 or large T, $0 < b_2 < 4/3$ and the minimizing solution is given by $a = 1$, which is the solution where both vehicles finish with the same final mass. Similarly, for sufficiently small α_0 or small T, $b_2 > 4/3$ and the optimal cooperative rendezvous requires one vehicle to provide the majority of thrusting.

To display some numerical results, consider Tables 1 and 2, which show the total propellant consumed for the optimal

Table 1 Cooperative and noncooperative rendezvous cost comparison for CW linearized gravity field with $\Delta r_0 = 0.0$

Case	α_0	ϕ_0	T	ΔM_c	ΔM_n	Savings, %
1	0.129	$\pi/4$	π	0.3126274	0.4256500	26.55
2	0.129	$\pi/2$	π	0.7336209	0.7477547	1.89
3	0.129	π	π	0.9217836	0.9222249	0.05
4	0.129	$\pi/4$	2π	0.0098561	0.0194250	49.26
5	0.129	$\pi/2$	2π	0.0388500	0.0734212	47.09
6	0.129	π	2π	0.1468426	0.2406734	38.99
7	3.668	$\pi/4$	π	0.0129475	0.0254016	49.03
8	3.668	$\pi/2$	π	0.0508033	0.0944120	46.19
9	3.668	π	π	0.1888240	0.2942934	35.84
10	3.668	$\pi/4$	2π	0.0003483	0.0006962	49.97
11	3.668	$\pi/2$	2π	0.0013924	0.0027790	49.90
12	3.668	π	2π	0.0055580	0.0110242	49.58
13	56.6	$\pi/4$	π	0.0008487	0.0016862	49.67
14	56.6	$\pi/2$	π	0.0033724	0.0067110	49.75
15	56.6	π	π	0.0134219	0.0263141	48.99
16	56.6	$\pi/4$	2π	0.0000227	0.0000451	49.67
17	56.6	$\pi/2$	2π	0.0000903	0.0001806	50.00
18	56.6	π	2π	0.0003611	0.0007219	49.98

Table 2 Cooperative and noncooperative rendezvous cost comparison for CW linearized gravity field with $\Delta r_0 = -0.1$

Case	α_0	ϕ_0	T	ΔM_c	ΔM_n	Savings, %
19	0.129	0	π	0.03704	0.07018	47.2
20	0.129	0.075π	π	0.00438	0.00870	49.7
21	0.129	0.15π	π	0.03704	0.07018	47.2
22	0.129	$\pi/2$	π	0.65442	0.68260	4.1
23	0.129	π	π	0.90968	0.91035	0.1
24	0.129	$3\pi/2$	π	0.78971	0.79713	0.9
25	0.129	0	2π	0.00433	0.00860	49.7
26	0.129	0.075π	2π	0.00166	0.00331	49.9
27	0.129	0.15π	2π	0.00077	0.00154	50.0
28	0.129	$\pi/2$	2π	0.01998	0.03880	48.5
29	0.129	π	2π	0.10899	0.18735	41.8
30	0.129	$3\pi/2$	2π	0.06551	0.11930	45.1

cooperative and active-passive rendezvous. The percentage of propellant saved by performing a cooperative rendezvous instead of a noncooperative one is also displayed. Table 1 considers rendezvous where both vehicles start in the same circular orbit ($\Delta r_0 = 0$). Table 2 displays costs for circular orbits where $\Delta r_0 = -0.1$. Because the gravity field is linearized and both vehicles are identical in their initial PTM ratios, the cost of either vehicle performing the entire maneuver is the same. Therefore only one active-passive rendezvous cost is listed. Also note that for Table 1, $0 < \phi_0 \leq \pi$. This is the only range needed because, with $\Delta r_0 = 0$, the cost associated with a rendezvous from the ϕ_0 phase is the same as the cost from the $-\phi_0$ phase; ΔM_c represents the cooperative cost and ΔM_n the noncooperative cost. Both vehicles begin the maneuver with an initial mass of 1 mass unit.

Table 1 shows that when the final maneuver time is fixed and $\Delta r_0 = 0$, the cost increases with ϕ_0 due to the additional thrusting needed to meet the rendezvous requirements. Both cooperative and noncooperative costs decrease as α_0 and T increase. Note that the cooperative rendezvous offers larger savings as α_0 and T increase. Table 2 shows that when $\Delta r_0 = -0.1$, the cost does not increase monotonically with ϕ_0; however, the cost continues to decrease as T increases. Also observe that increasing Δr_0 for a given ϕ_0, α_0, and T does not necessarily result in an increase in total propellant consumption as can be seen by comparing case 3 from Table 1 with case 23 in Table 2. In all cases, a cooperative rendezvous requires less total propellant to meet the rendezvous requirements.

From Tables 1 and 2 the limiting value in total mass savings that the cooperative rendezvous can offer over the noncooperative rendezvous appears to be 50%. For sufficiently large total maneuver time or large initial PTM ratios, this observation can be proven analytically.[12]

Consider Fig. 1, which displays the total propellant consumed during a cooperative rendezvous as a function of the initial phase angle ϕ_0 between the two vehicles. The total maneuver time is 2π TU and $\alpha_0 = 56.6$. One curve is the total propellant consumed for a rendezvous from the same circular orbit ($\Delta r_0 = 0.0$), and the second is the cost for a rendezvous between neighboring circular coplanar orbits where $\Delta r_0 = -0.1$. Total propellant consumption is plotted on a logarithmic scale. Calculated data points are represented by symbols that are connected by cubic splines. The cost curve associated with $\Delta r_0 = 0.0$ is cyclic with period 2π. Its minimum occurs at $\phi_0 = 0$ with a cost of 0 representing a completed rendezvous. This cost reaches its maximum value at π rad, the largest relative phase angle possible between two vehicles in the same orbit. The second cost curve is also cyclic; however, with $\Delta r_0 = -0.1$, the initial phase angle that results in the minimum cost is a nonzero angle $\phi_{0\min}$. As is the case with $\Delta r_0 = 0.0$, the cost achieves its maximum value at $\phi_{0\min} + \pi$ rad.

The total propellant consumed for a cooperative rendezvous between specified initial orbits decreases as the initial PTM ratio is increased; however, the initial phase angle that results in the minimum total propellant consumed $\phi_{0\min}$ is constant. The value of $\phi_{0\min}$ may be calculated through the cost functional associated with a cooperative rendezvous. The $\phi_{0\min}$ is determined through Eq. (49):

$$\frac{dJ}{d\phi_0} = \left(\frac{\partial J}{\partial a}\frac{\partial a}{\partial b_2} + \frac{\partial J}{\partial b_2}\right)\frac{\partial b_2}{\partial \phi_0} = 0 \tag{49}$$

which is satisfied if one of two conditions is met:

$$\frac{\partial J}{\partial a}\frac{\partial a}{\partial b_2} + \frac{\partial J}{\partial b_2} = 0 \tag{50}$$

or

$$\frac{\partial b_2}{\partial \phi_0} = \frac{c^T K}{\alpha_{10}}\Phi_{rp}^{-1}(T)\Phi_{rr}(T)[0\ 1\ 0\ 0\ 0\ 0]^T = 0 \tag{51}$$

In general, a ϕ_0 cannot be found that will satisfy Eq. (50). However, an expression for ϕ_0 that will satisfy Eq. (51) can be determined. For a cooperative rendezvous between neighboring circular orbits, a simple expression for $\phi_{0\min}$ can be obtained[12]:

$$\phi_{0\min} = -\tfrac{3}{4}T\Delta r_0 \tag{52}$$

Note that Eq. (52) is independent of the initial PTM ratios for the vehicles. From Eq. (52), the value of $\phi_{0\min}$ with $\Delta r_0 = -0.1$ and $T = 2\pi$ is calculated as 0.15π or 0.4712... rad. This $\phi_{0\min}$ agrees with the cost curve presented in Fig. 1.

A useful feature of a cooperative rendezvous is the ability to predict the final orbit. From Eq. (38) it can be shown that the final orbit after a cooperative rendezvous between neighbor-

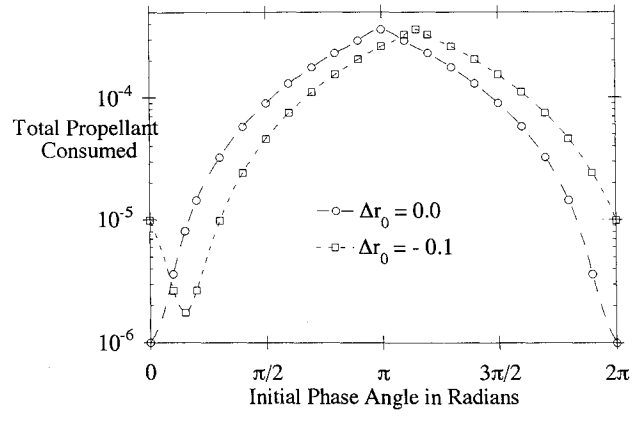

Fig. 1 Total propellant consumed vs phase angle: $\alpha_0 = 56.6$.

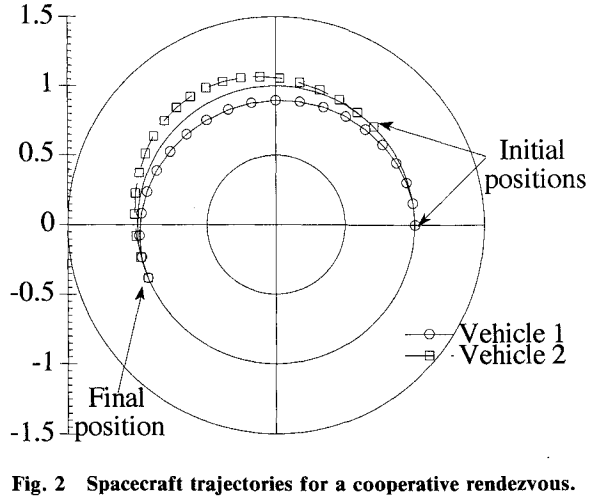

Fig. 2 Spacecraft trajectories for a cooperative rendezvous.

Table 3 Cost comparison for cooperative and noncooperative neighboring inclined circular rendezvous

α_0	T	ΔM_c	ΔM_n
0.129	π	2.4724×10^{-2}	4.76864×10^{-2}
0.129	2π	5.2391×10^{-3}	1.0396×10^{-2}
3.668	π	8.8014×10^{-4}	1.7580×10^{-3}
3.668	2π	1.8472×10^{-4}	3.6934×10^{-4}
56.6	π	5.7061×10^{-5}	1.1441×10^{-4}
56.6	2π	1.1972×10^{-5}	2.3943×10^{-5}

ing circular, coplanar orbits is itself a neighboring circular, coplanar orbit. This final circular orbit has an intermediate radius and phase angle as measured with respect to the rotating reference frame:

$$\begin{bmatrix} \delta r_i(T) \\ \delta \dot{r}_i(T) \end{bmatrix} = -\frac{a^2}{b_3 + a^2} \Phi_{rr}(T) \times [\Delta r_0 \quad -\phi_0 - (3/2)T\Delta r_0 \quad 0 \quad 0 \quad -(3/2)\Delta r_0 \quad 0]^T \tag{53}$$

Figure 2 displays the position trajectories for a cooperative coplanar rendezvous. The initial orbits each have a radius of 1 DU, and the initial phase angle is $\phi_0 = \pi/4$. The total maneuver time is π TU, and the initial PTM ratio is 0.129. For this maneuver, the optimal cooperative solution is for both vehicles to use the same amount of propellant, i.e., $a = 1$. As Eq. (53) predicts, the cooperative rendezvous finishes with an angle of $\pi/8$ measured with respect to the rotating reference frame whose origin initially coincides with vehicle 1's position. Therefore, each vehicle removes half of the original phase angle. Figure 2 also shows that to rendezvous vehicle 1 must increase its velocity by decreasing its radius, whereas vehicle 2 decreases its velocity by increasing its radius.

Neighboring Inclined Rendezvous Results

A cooperative rendezvous between inclined circular orbits whose difference in in-plane and out-of-plane (OOP) motion is relatively small is considered. The effect of varying the initial PTM ratio α_0 and the total rendezvous time T on total propellant consumption between inclined circular orbits is similar to the coplanar results as illustrated in Table 3. For these cases, the initial orbits differ in orbital radius $\Delta r_0 = -0.07071$ DU and initial OOP displacement $\Delta z_0 = z_{10} - z_{20} = -0.07071$ DU with zero initial phase angle. Table 3 indicates that as T increases, the cost of the rendezvous decreases. Also, as α_0 is increased, the relative efficiency of the engines increases and the cost decreases. In all cases, the cooperative cost is less than the noncooperative cost. As T and α_0 increase, the percentage of savings that a cooperative rendezvous can offer over an active-passive rendezvous approaches the limiting value of 50%.[12]

Next, consider Fig. 3, which displays the total propellant consumed during a cooperative and noncooperative rendezvous as a function of the difference in the initial in-plane phase angle ϕ_0 between the two vehicles. The total maneuver time is 2π TU and $\alpha_0 = 3.668$. The initial difference in the in-plane and OOP displacement used for the study was $\Delta x_0 = \Delta z_0 = -0.07071$ DU. Figure 3 shows that the cooperative and noncooperative cost curves as a function of initial phase angle are similar in form. Each curve achieves its minimum value at the same $\phi_{0\min}$ and its maximum value at $\phi_{0\min} + \pi$ rad. This characteristic is easily explained by examining the derivative of the noncooperative cost functional with respect to the initial phase angle:

$$\frac{dJ_n}{d\phi_0} = \frac{\partial J_n}{\partial b_2}\frac{\partial b_2}{\partial \phi_0} = \left[\frac{m_{10}b_3}{(b_1 + b_2)^2}\right]\frac{\partial b_2}{\partial \phi_0} = 0 \tag{54}$$

Equation (54) is satisfied by

$$[m_{10}b_3/(b_1 + b_2)^2] = 0 \tag{55}$$

or

$$\frac{\partial b_2}{\partial \phi_0} = 0 \tag{56}$$

No ϕ_0 exists that will satisfy Eq. (55). Equation (56) is the same equation that defines $\phi_{0\min}$ for a cooperative rendezvous, Eq. (51). Therefore, the same initial ϕ_0 minimizes total propellant consumption for both cooperative and noncooperative rendezvous.

Another feature common to both coplanar and inclined cooperative rendezvous is the ability to predict the final orbit after the rendezvous. Equation (57) shows that a cooperative rendezvous between neighboring circular inclined orbits terminates in a neighboring circular inclined final orbit. For equally efficient vehicles ($b_3 = 1$) with sufficiently large total transfer times ($a = 1$), the terminal orbit has an inclination and orbital radius that lies midway between the initial orbits:

$$\begin{bmatrix} \delta r_i(T) \\ \delta \dot{r}_i(T) \end{bmatrix} = -\frac{a^2}{b_3 + a^2} \Phi_{rr}(T) \times [\Delta r_0 \quad -\phi_0 - (3/2)T\Delta r_0 \quad \Delta z_0 \quad 0 \quad -(3/2)\Delta r_0 \quad \Delta \dot{z}_0]^T \tag{57}$$

Figures 4 and 5 display the trajectories for a cooperative rendezvous from inclined circular orbits with $\Delta x_0 = \Delta z_0 = -0.07071$ DU, $\phi_0 = \pi$ rad, $T = 2\pi$ TU, and $\alpha_0 = 3.668$. During this maneuver, both vehicles use identical amounts of

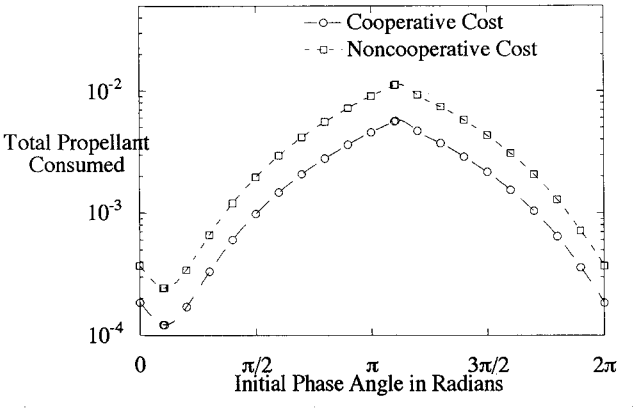

Fig. 3 Total propellant consumed vs phase angle for cooperative and active-passive rendezvous from neighboring inclined circular orbits.

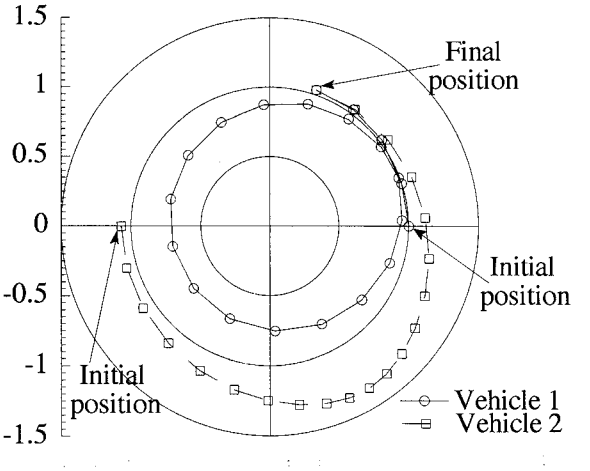

Fig. 4 In-plane spacecraft trajectories for a cooperative rendezvous.

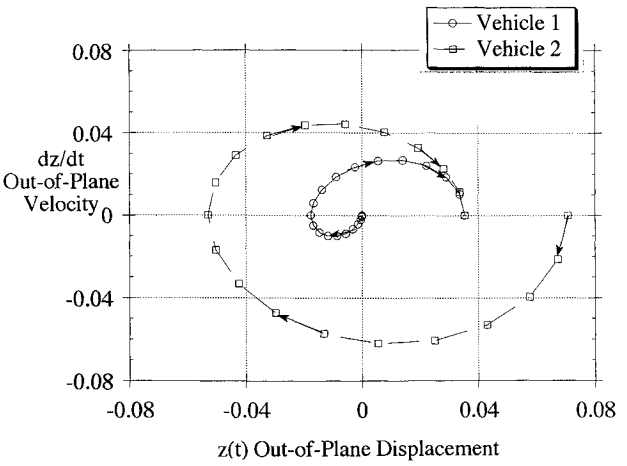

Fig. 5 Phase space trajectories for a cooperative rendezvous.

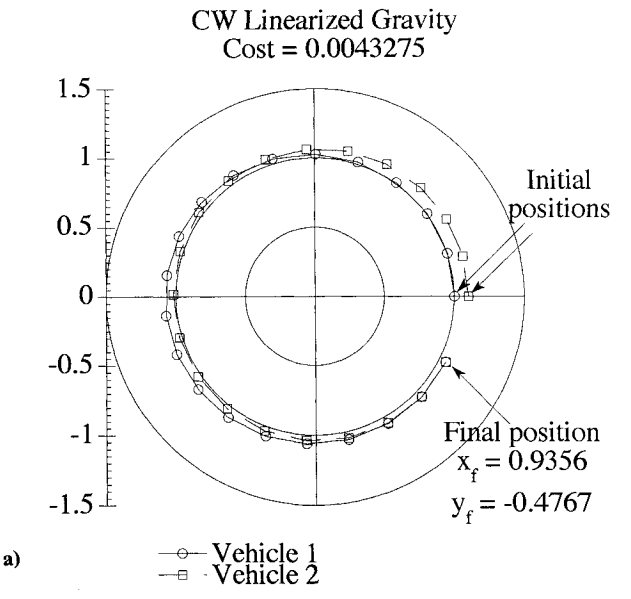

a)

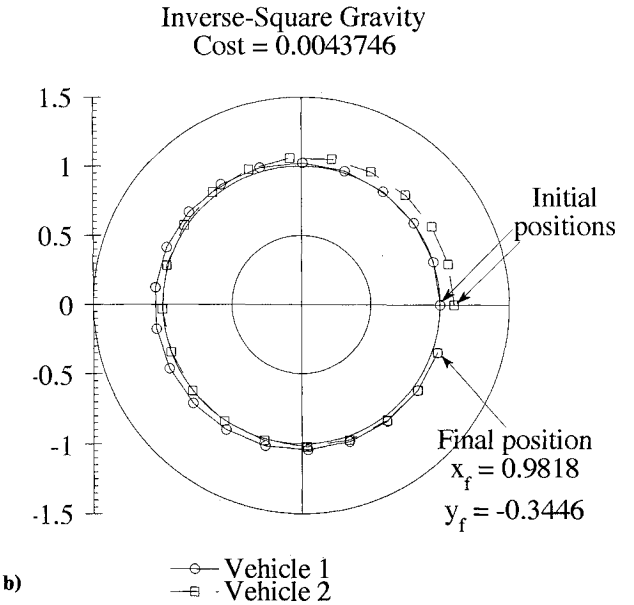

b)

Fig. 6 Hill-Clohessy-Wiltshire and inverse-square gravity cooperative rendezvous trajectories.

propellant, i.e., $a = 1$. Equation (57) yields a circular terminal orbital radius of 1.035 DU and a final phase angle of 0.3939π rad. Figure 4 shows the in-plane motion. To rendezvous, vehicle 1 increases its velocity by decreasing its radius, whereas vehicle 2 decreases its velocity by increasing its radius. Figure 5 displays the OOP phase space trajectories. For the OOP motion, it is convenient to plot the position and velocity of the vehicles in phase space where the position is measured along the abscissa and the velocity along the ordinate. In this space, vehicle 1's initial orbit begins at the origin, and vehicle 2's initial orbit is circular with radius $\sqrt{\Delta z_0^2 + \Delta \dot{z}_0^2}$ centered at the origin. Vehicle 1 moves in a counterclockwise direction from the origin to the final circular orbit of radius 0.03536. Vehicle 2 leaves its circular orbit at a radius of 0.07071 in a counterclockwise direction and also terminates in a circular orbit of 0.03536. The rendezvous point in the phase space is at (0.03536, 0). Since the relative inclination between the two vehicles is small, a three-dimensional plot greatly resembles the in-plane trajectories of Fig. 4.

A comparison between optimal cooperative rendezvous solutions obtained analytically for the linearized gravity field and numerically generated results for the inverse-square gravity field was considered in Ref. 12. If the trajectories of both spacecraft remain relatively close to the reference orbit, the results are very similar. However, as the trajectories deviate significantly from the reference orbit and leave the linear range, discrepancies between the solutions begin to appear. In such cases, the inverse-square gravity model is required to yield accurate results. Figure 6 displays optimal cooperative rendezvous trajectories for both gravity models where $\alpha_0 = 0.129$, $T = 2\pi$ TU, $\phi_0 = 0$, and $\Delta r_0 = -0.1$ DU.

Concluding Remarks

Analytical solutions describing both active-passive and cooperative rendezvous for power-limited spacecraft in the Hill-Clohessy-Wiltshire linearized gravity field have been supplied. In the case of equal initial power-to-mass ratios and circular initial orbits, cooperative rendezvous can offer considerable savings in total propellant consumption over an active-passive rendezvous. The savings increase with initial power-to-mass ratio of the vehicles and with total maneuver time.

Appendix

The partitions to the state transition matrix and the K matrix of Eq. (31) for the Hill-Clohessy-Wiltshire linearized gravity model appear next. The mean motion n has been normalized to one. Define s to be the elapsed time $s = t - t_0$:

$$\phi_{rr}(s) = \Phi_{pp}(s) = \begin{bmatrix} M(s) & N(s) \\ S(s) & T(s) \end{bmatrix}$$

where

$$M(s) = \begin{bmatrix} 4 - 3\cos(s) & 0 & 0 \\ 6[\sin(s) - s] & 1 & 0 \\ 0 & 0 & \cos(s) \end{bmatrix}$$

$$N(s) = \begin{bmatrix} \sin(s) & 2[1 - \cos(s)] & 0 \\ -2[1 - \cos(s)] & 4\sin(s) - 3s & 0 \\ 0 & 0 & \sin(s) \end{bmatrix}$$

$$S(s) = \begin{bmatrix} 3\sin(s) & 0 & 0 \\ -6[1 - \cos(s)] & 0 & 0 \\ 0 & 0 & -\sin(s) \end{bmatrix}$$

$$T(s) = \begin{bmatrix} \cos(s) & 2\sin(s) & 0 \\ -2\sin(s) & 4\cos(s) - 3 & 0 \\ 0 & 0 & \cos(s) \end{bmatrix}$$

$$\Phi_{rp}(s) = \begin{bmatrix} U(s) & V(s) \\ W(s) & X(s) \end{bmatrix}$$

$$U(s) = \begin{bmatrix} 28 - 28\cos(s) - 6s^2 - (15/2)s\sin(s) & -2\sin(s) + 2s & 0 \\ -50s + 65\sin(s) + 3s^2 - 15s\cos(s) & -(3/2)s^2 + 4 - 4\cos(s) & 0 \\ 0 & 0 & (1/2)s\sin(s) \end{bmatrix}$$

$$V(s) = \begin{bmatrix} (13/2)\sin(s) - 4s - (5/2)s\cos(s) & 16 - 3s^2 - 16\cos(s) - 5s\sin(s) & 0 \\ -16 + 3s^2 + 16\cos(s) + 5s\sin(s) & (3/2)s^3 + 38\sin(s) - 28s - 10s\cos(s) & 0 \\ 0 & 0 & (1/2)\sin(s) - (1/2)s\cos(s) \end{bmatrix}$$

$$W(s) = \begin{bmatrix} (41/2)\sin(s) - 12s - (15/2)s\cos(s) & 2 - 2\cos(s) & 0 \\ -50 + 50\cos(s) + 9s^2 + 15s\sin(s) & -3s + 4\sin(s) & 0 \\ 0 & 0 & (1/2)\sin(s) + (1/2)s\cos(s) \end{bmatrix}$$

$$X(s) = \begin{bmatrix} -4 + 4\cos(s) + (5/2)s\sin(s) & 11\sin(s) - 6s - 5s\cos(s) & 0 \\ -11\sin(s) + 6s + 5s\cos(s) & (9/2)s^2 - 28 + 28\cos(s) + 10s\sin(s) & 0 \\ 0 & 0 & (1/2)s\sin(s) \end{bmatrix}$$

$$K = \int_{t_0}^{tf} \Phi_{pp}^T(t) \begin{bmatrix} I_3 & 0_3 \\ 0_3 & 0_3 \end{bmatrix} \Phi_{pp}(t)\, dt$$

$$K(T) = \begin{bmatrix} K_1(T) & K_2(T) \\ K_2^T(T) & K_3(T) \end{bmatrix}$$

$$T = t_f - t_0$$

$$K_1(T) = \begin{bmatrix} K_{111}(T) & K_{112}(T) & K_{113}(T) \\ K_{121}(T) & K_{122}(T) & K_{123}(T) \\ K_{131}(T) & K_{132}(T) & K_{133}(T) \end{bmatrix}$$

$$K_{111}(T) = (77/2)T - (27/4)\sin(2T) + 12T^3 - 72T\cos(T) - 96\sin(T)$$

$$K_{112}(T) = K_{121}(T) = -3[T^2 + 2\cos(T)] + 6$$

$$K_{122}(T) = T$$

$$K_{133}(T) = (1/2)\sin(T)\cos(T) + (1/2)T$$

$$K_{113}(T) = K_{123}(T) = K_{131}(T) = K_{132}(T) = 0$$

$$K_2(T) = \begin{bmatrix} K_{211}(T) & K_{212}(T) & K_{213}(T) \\ K_{221}(T) & K_{222}(T) & K_{223}(T) \\ K_{231}(T) & K_{232}(T) & K_{233}(T) \end{bmatrix}$$

$$K_{211}(T) = 6T^2 - 4\cos(T) - (9/2)\cos^2(T) - 12T\sin(T) + (17/2)$$

$$K_{212}(T) = 23T + 6T^3 + 42T\cos(T) - (9/2)\sin(2T) - 56\sin(T)$$

$$K_{221}(T) = 2[\sin(T) - T]$$

$$K_{222}(T) = -(3/2)T^2 - 4\cos(T) + 4$$

$$K_{223}(T) = (1/2)\sin^2(T)$$

$$K_{233}(T) = K_{223}(T) = K_{231}(T) = K_{232}(T) = 0$$

$$K_3(T) = \begin{bmatrix} K_{311}(T) & K_{312}(T) & K_{313}(T) \\ K_{321}(T) & K_{322}(T) & K_{323}(T) \\ K_{331}(T) & K_{332}(T) & K_{333}(T) \end{bmatrix}$$

$$K_{311}(T) = (13/2)T - 8\sin(T) + (3/4)\sin(2T)$$

$$K_{312}(T) = K_{321}(T) = 3T^2 - 3\cos^2(T) - 6T\sin(T) + 3$$

$$K_{322}(T) = 3T^3 + 24T\cos(T) + 14T - 3\sin(2T) - 32\sin(T)$$

$$K_{333}(T) = (1/2)T - (1/2)\cos(T)\sin(T)$$

$$K_{313}(T) = K_{323}(T) = K_{331}(T) = K_{332}(T) = 0$$

Acknowledgments

This research was supported partially through an Amelia Earhart Fellowship sponsored by ZONTA International and partially through a NASA Fellowship.

References

[1]Meschler, P. A., "Time-Optimal Rendezvous Strategies," *IEEE Transactions on Automatic Control,* Vol. 8, No. 10, 1963, pp. 279–282.

[2]Gieseking, K. L., "Optimal Control of Co-Operative Systems: The Rendezvous Problem," Univ. of Illinois at Urbana-Champaign, Coordinated Science Lab., Rept. R-218, Urbana, IL, 1964.

[3]Carter, T. E., "A Simple Feedback Law for a Cooperative Rendezvous Problem," NASA TM X-53568, Oct. 1966.

[4]Kahne, S. J., "Optimal Cooperative State Rendezvous and Pontryagin's Maximum Principle," Air Force Cambridge Research Labs., AFCRL-65-233, Hanscom Field, Bedford, MA, April 1965.

[5]Prussing, J. E., and Conway, B. A., "Optimal Terminal Maneuver for a Cooperative Impulsive Rendezvous," *Journal of Guidance, Control, and Dynamics,* Vol. 12, No. 3, 1989, pp. 433–435.

[6]Mirfakhraie, K., "Optimal Cooperative Time-Fixed Impulsive Rendezvous," Ph.D. Thesis, Univ. of Illinois at Urbana-Champaign, Urbana, IL, 1991.

[7]Mirfakhraie, K., and Conway, B. A., "Optimal Cooperative Time-Fixed Impulsive Rendezvous," AIAA/AAS Astrodynamics Conference, AIAA Paper 90-2962, Portland, OR, Aug. 1990.

[8]Prussing, J. E., "Equation for Optimal Power-Limited Spacecraft Trajectories," *Journal of Guidance, Control, and Dynamics,* Vol. 16, No. 2, 1993, pp. 391–393.

[9]Bryson, A. E., and Ho, Y., *Applied Optimal Control,* Hemisphere, New York, 1975, Chap. 2.

[10]Lawden, D. F., *Optimal Trajectories for Space Navigation,* Butterworths, London, England, UK, 1963, Chap. 3.

[11]Prussing, J. E., and Conway, B. A., *Orbital Mechanics,* Oxford Univ. Press, New York, 1993.

[12]Coverstone-Carroll, V., "Optimal Cooperative Power-Limited Rendezvous," Ph.D. Thesis, Univ. of Illinois at Urbana-Champaign, Urbana, IL, 1992.

[13]Coverstone-Carroll, V., and Prussing, J. E., "Optimal Cooperative Power-Limited Rendezvous," AAS/AIAA Astrodynamics Specialist Conference, AAS Paper 91-444, Durango, CO, Aug. 1991.